AIAA Guidance, Navigation, and Control Conference and Exhibit
15 - 18 August 2005, San Francisco, California

AIAA 2005-6243

Low-Power, High-Agility Space Robotics

Mason A. Peck*
Cornell University, Ithaca, NY, 14852

Control-moment gyroscopes (CMGs) have been used for attitude control on spacecraft that require large torques. We propose them for use in multibody robotic systems where high agility (or dexterity) and low power are important design goals. The architecture we propose offers singularity-free, reactionless slewing of a multi-joint robotic arm. It promises one to two orders of magnitude reduction in electromechanical power over otherwise identical systems with traditional joint drives or reactionless rotors. In broad terms, this improvement is possible because the CMGs transfer momentum with only small changes in kinetic energy. The large torques with which CMGs are associated are, in fact, constraint torques if the bodies are rigidly connected. They do no work, and they therefore require no input power per se. We describe the implementation of this concept on a small, free-flying spacecraft-maintenance robot (proposed by Princeton Satellite Systems), where 2 rad/sec rate, 2 rad/sec acceleration, and 2 rad/sec jerk are achieved for less than 1 kW peak power.

Nomenclature

P_s	=	shaft power
$\boldsymbol{\tau}_i$	=	torque applied by the i^{th} CMG or scissored pair of CMGs
$\boldsymbol{\omega}$	=	pressure coefficient
ϕ_i	=	gimbal angle of the i^{th} CMG
$\boldsymbol{h}_{ri}$	=	rotor angular momentum vector for the i^{th} CMG
$\boldsymbol{h}_i$	=	angular momentum of
$\boldsymbol{a}_i$	=	joint axis (unit vector) of the i^{th} body the i^{th} CMG or scissored pair of CMGs
$\boldsymbol{\omega}^{i/N}$	=	the i^{th} body's angular-velocity vector in an inertial frame N
$\boldsymbol{\omega}^{i/j}$	=	the angular velocity of a frame fixed in the i^{th} body relative to a frame fixed in the j^{th} body
$\hat{\boldsymbol{g}}_i$	=	i^{th} CMG's gimbal axis
θ_i	=	gimbal angle of the i^{th} CMG or scissored pair of CMGs
${}^{C}v$	=	3×1 matrix of measure numbers of the vector $\boldsymbol{v}$ along basis vectors fixed in frame C
$v^{\times}$	=	3×3 matrix equivalent of the cross product operation using the vector $\boldsymbol{v}$
$\overset{i}{\boldsymbol{v}}$	=	vector derivative of the vector $\boldsymbol{v}$ in frame i
$\hat{\boldsymbol{r}}_i$	=	i^{th} CMG rotor's spin axis
Ω_{ri}	=	magnitude of the i^{th} CMG rotor's angular velocity in a gimbal-fixed frame (its spin rate)
E_{joints}	=	kinetic energy of the joints
E_{ACS}	=	kinetic energy in the attitude-control system reaction-wheel array

I. Introduction

CONTROL-MOMENT gyroscopes (CMGs) have been used for attitude control on spacecraft that require large torques. A CMG consists of a spinning rotor and one or more motorized gimbals that tilt the rotor's angular momentum. As the rotor tilts, the changing angular momentum causes a gyroscopic torque that rotates the spacecraft. Figure 1 is a picture of the Honeywell M50 CMG, which produces 50 ft-lb with 50 ft-lb-sec rotor on a 1 rad/sec gimbal. Achieving this peak torque requires an astonishingly low 120W.[1]

* Assistant Professor, Sibley School of Mechanical and Aerospace Engineering, 212 Upson Hall, Member AIAA.

Figure 1. Honeywell M50 CMG

CMGs have been used for decades in large spacecraft, including Skylab and the International Space Station. These large spacecraft have implemented dual-gimbal CMGs, which do not offer the power, torque, and robustness benefits of the single-gimbal CMGs envisioned for the maintenance bot. In the years to come single-gimbal CMGs will provide attitude control for several commercial earth-imaging satellites, such as Lockheed-Martin's Ikonos and Ball Aerospace's WorldView spacecraft. We propose to base the design of the CMGs for the maintenance bot on the technology of Honeywell Defense and Space Electronics Systems, whose high-reliability and high technology-readiness CMGs boast an unrivaled history of mission success.

A CMG is far more power efficient than the conceptually simpler and more commonly used reaction wheel (RWA). An RWA applies torque simply by changing its rotor spin speed ω, but in doing so imparts shaft power P_s:

$$P_s = \boldsymbol{\tau} \cdot \boldsymbol{\omega}, \tag{1}$$

a result that assumes an entirely mechanical, lossless system. The scalar P_s is the projection of the vector motor torque $\boldsymbol{\tau}$ onto the rotor angular-velocity vector $\boldsymbol{\omega}$. In contrast, a CMG's gimbal motor is roughly orthogonal to the rotor spin axis, and the resulting shaft power is virtually zero if the gimbal inertia and the motor losses are negligible. For a few hundred Watts and about 100 kg of mass, large CMGs have produced thousands of Nm of torque, enough to flip over an SUV[2]. A reaction wheel of similar capability would require megawatts of power to produce torque at speed, simply because the torque is aligned with the spin axis.

II. Robotic System Architecture

Operating either a CMG or an RWA produces a torque that reacts onto the spacecraft body, influencing the spacecraft angular momentum. The difference is that the CMG's own angular momentum changes in direction (but not in magnitude), while the RWA's angular momentum changes in magnitude (but not in direction). If the CMG's gimbal is rigid, the gyroscopic torque for which a CMG is responsible is purely a constraint torque. As such, it does no work. At the heart of this surprising result is the counterintuitive fact that one can alter the distribution of momentum among bodies in a dynamical system in a way that is independent of energy. That is, changing the angular momentum of various links in the maintenance bot system can be done in a way that requires no energy except what is lost through electromechanical inefficiencies. Using CMGs is a natural way to realize such an architecture.

Momentum-storage devices (to date, exclusively reaction wheels) have been used to provide "reactionless" motion of high-agility gimbals and entire spacecraft payloads. Although other forms of reactionless steering have been proposed[3], this one depends on internal gyricity. The principle of operation is simple: rather than using a motor that reacts the drive torque of a moving component back onto the spacecraft bus, where it must be dealt with as an attitude disturbance, a reactionless drive absorbs the momentum internally. For example, a gimbal may be

actuated by an RWA (realized, perhaps, as a circumferential ring) aligned with the gimbal axis. When the RWA spins up in one direction, the gimbal spins up in the other. The concept is shown in Figure 2.

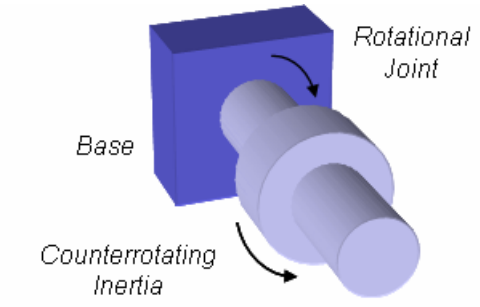

Figure 2. Schematic of a Reactionless Jointed System

One can generalize this single-axis principle to multiple degrees of freedom associated with a spacecraft payload: a collection of RWAs manages the entire payload's angular-momentum state in three degrees of freedom, so that the payload may undergo attitude motions that are largely imperceptible to the rest of the spacecraft. Such an architecture simplifies design and integration because payload components may be developed independently, without the risk of unwanted interactions after the system is built. It also simplifies operations. Many tasks can be undertaken simultaneously with virtually no coupling between physical behaviors or tasking. In the case of the maintenance bot, these tasks may include simultaneously manipulating many different components of a spacecraft under repair.

Reactionless benefits come with the territory for the CMG-driven maintenance bot. Here, incorporating CMGs throughout the kinematic chain of links provides not only high-torque actuation but also inherent reactionless dynamics. When a joint is actuated, the torque comes not from a direct-drive motor that interacts with its neighboring body but from manipulating the distribution of momentum among the CMGs and the body to which they are mounted. Perhaps the most important impact of reactionless CMG-based control is that it requires only 1%-10% the electrical power for a comparable RWA-based or joint-driven robotic system, as we explain in this section. This feature enables high agility (or dexterity) for modest power or typical agility for considerable power savings over existing robotic concepts. Low power improves the robustness and safety of the maintenance-bot system, and the resulting cost and mass savings likely roll up to the system level.

Although many CMG arrangements are possible, our baseline concept includes a scissored pair of CMGs for each rotational joint in the maintenance bot. A scissored pair is an array of two CMGs with parallel gimbal axes and opposite angular velocities. Equivalently, a scissored pair may be said to consist of two CMGs with antiparallel gimbal axes and equal angular velocities. Figure 3 is a sketch of the concept. The scissored-pair arrangement ensures that the sum of the CMGs' angular momentum aligns with a single axis, like that of a reaction wheel, which drastically simplifies the control algorithms. As Figure 3 indicates, the CMG gimbal angles ϕ_1 and ϕ_2 are kept constant, either through mechanical means such as gears or through closed-loop control. Although the individual CMGs' angular-momentum vectors $\boldsymbol{h}_{r1}$ and $\boldsymbol{h}_{r2}$ tilt away from the rotational joint's axis $\boldsymbol{a}$, their sum remains aligned with $\boldsymbol{a}$. Thus, the momentum exchange from the CMG to the jointed body accelerates the body about its joint axis only, without coupling into the rest of the base body A.

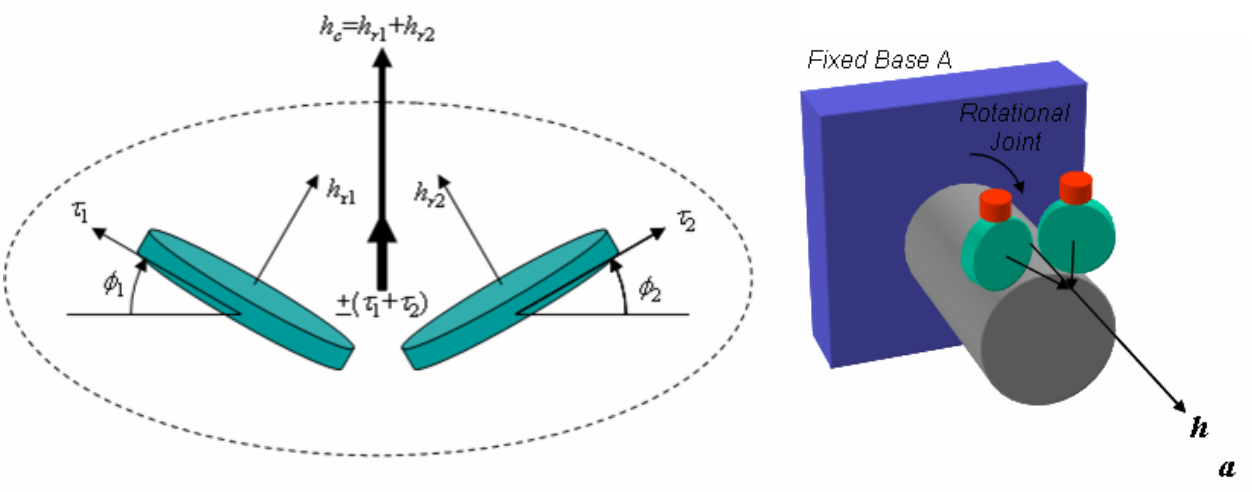

Figure 3. Scissored Pair of CMGs and Implementation on a Single-DOF Jointed Body

The robotic arm(s) of the maintenance bot may consist of many such jointed bodies. A schematic is shown in Figure 4, where the end effector is represented as a black cone (perhaps suggesting the sun shield for the lens of an inspection camera).

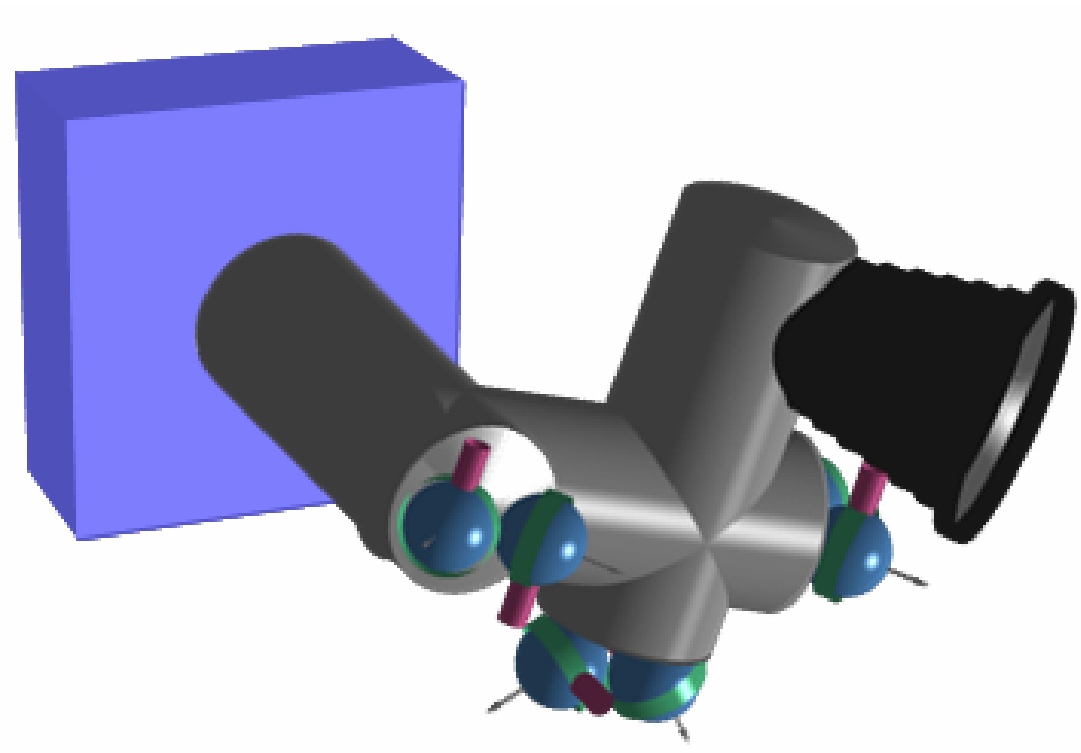

Figure 4. Three-body Robotic Arm, Each Joint Actuated by a Scissored Pair of CMGs

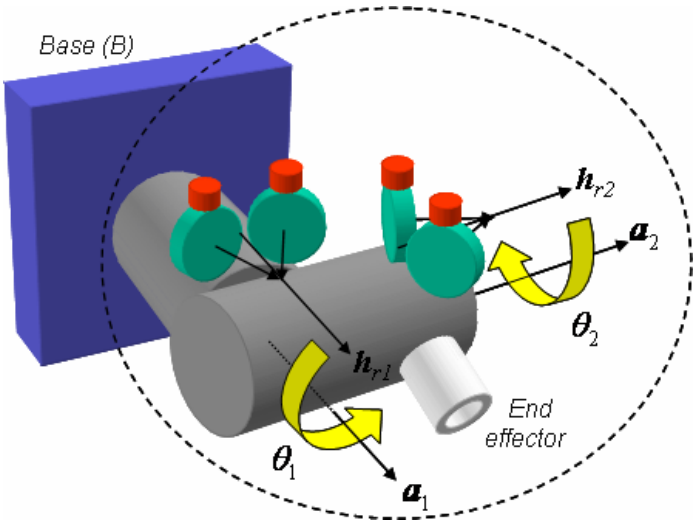

Figure 5. Two-Link Example with Two Scissored Pairs of CMGs

If necessary, the base body can be driven by suite of four identical CMGs. This choice allows a single mathematical degree of freedom for singularity avoidance, providing a singularity-free region of operation within a $2h_r$ sphere, where h_r is the momentum of an individual CMG's rotor in the base body. The details of the singularity-avoidance method are not presented here.

The low-power benefits of CMGs are most effectively realized in a system where the CMG base's angular-velocity vector does not cause gyroscopic torques along the CMG gimbal axes, which would introduce large holding-torque requirements on the gimbal motors. Conversely, reactionless control of outboard joints virtually eliminates control power required on inboard joints (and the base body). For example, consider a situation in which a joint rotates about an inertial axis that is perpendicular to the CMG momentum vector and to the CMG gimbal axis. In the case of the single body in Figure 3, one such axis is the joint axis when the CMG has rotated about its gimbal roughly 90^o from the orientation shown. Such rotation applies torque back onto the CMG gimbal motor, which the motor then must react. Unless the motor has some mechanical anti-backlash device (like a ratchet), the motor must apply this torque through electrical power in its windings with all the related losses and impacts to harness design.

III. Fault Robustness

A. Impact Memory

If the robotic system described here interacts with other bodies, it retains a record of these interactions. One might call it an impact memory. Specifically, the moments applied by the robotic system during contact alter the system angular momentum. In a space system, where environmental torques may be negligibly small, these moments may accurately represent a record of unwanted contact, in which case operators can evaluate the history of the impacts by looking at the angular momentum embedded in the CMGs and the links. If the contact is planned—for example, as part of an in-orbit construction procedure—looking at the embedded momentum has other benefits. Among them, the altered angular-momentum state can be used to verify that appropriate manipulations were carried out. Perhaps even more interesting, manipulating another object and recording the kinematic time history along with the robotic system's momentum may be used to identify the object's mass properties[4].

B. CMG Failures

The maintenance bot architecture can accommodate a variety of approaches to subsystem fault tolerance. With regard to CMG failures or underperformance, we propose a concept in which the base body attitude control is coupled to the joint attitude control to minimize power (or keep power within constraints for degraded agility). Again, the power-optimal design is one that includes reactionless control of the joints. However, in a multibody system without reactionless control, it is possible to describe constraints on the motion such that a steering algorithm can minimize power. A detailed explanation follows.

We consider the case of n jointed bodies, each of which is driven by a single CMG. The scissored-pair configuration is subject to the same constraints, but the example is clearer for single CMGs, and therefore we proceed with the simpler case. Let $\boldsymbol{\omega}^{\mathrm{i/N}}$ represent the i^{th} body's angular-velocity vector in an inertial frame N. Let $\hat{\boldsymbol{g}}_i$ represent the i^{th} CMG's gimbal axis, and let $\boldsymbol{h}_{ri}$ represent the i^{th} CMG's angular-momentum vector. The angle ϕ_i is the i^{th} CMG's gimbal axis, taken to be zero when $\boldsymbol{h}_i \parallel \hat{\boldsymbol{a}}_i$, the i^{th} body's joint axis. We define a frame B that rotates with the base body (the central body of the maintenance bot). The total angular velocity of the i^{th} body is then the sum of the joint rates along the kinematic chain back to the base body, whose inertial angular velocity is $\boldsymbol{\omega}^{\mathrm{B/N}}$:

$$\boldsymbol{\omega}^{\mathrm{i/N}} = \boldsymbol{\omega}^{\mathrm{i/i\text{-}1}} + \boldsymbol{\omega}^{\mathrm{i\text{-}1/i\text{-}2}} + \ldots + \boldsymbol{\omega}^{2/1} + \boldsymbol{\omega}^{1/\mathrm{B}} + \boldsymbol{\omega}^{\mathrm{B/N}}. \tag{2}$$

We assume that the CMG gimbal axes are perpendicular to the joint axes (i.e. $\hat{\boldsymbol{g}}_i \perp \hat{\boldsymbol{a}}_i$. Expressed algebraically, the requirement for minimum power is then

$$\left(\boldsymbol{\omega}^{\mathrm{i/N}} \times \boldsymbol{h}_{ri}\right) \cdot \hat{\boldsymbol{g}}_i = 0, \tag{3}$$

i.e., the projection of the gyroscopic torque due to the inertial rate of the joint onto the CMG gimbal axis is zero. Writing these constraints for all of the joints in the system results in n equations in the n joint angular rates $\dot{\theta}$.

$$\begin{bmatrix} \|\boldsymbol{h}_{rn}\|\sin\phi_n & \hat{\boldsymbol{g}}_n \cdot \left(\boldsymbol{h}_{rn} \times \boldsymbol{a}_{n-1}\right) & \hat{\boldsymbol{g}}_n \cdot \left(\boldsymbol{h}_{rn} \times \boldsymbol{a}_{n-2}\right) & \cdots & \hat{\boldsymbol{g}}_n \cdot \left(\boldsymbol{h}_{rn} \times \boldsymbol{a}_1\right) \\ \|\boldsymbol{h}_{rn-1}\|\sin\phi_{n-1} & 0 & \hat{\boldsymbol{g}}_{n-1} \cdot \left(\boldsymbol{h}_{rn-1} \times \boldsymbol{a}_{n-2}\right) & \cdots & \hat{\boldsymbol{g}}_{n-1} \cdot \left(\boldsymbol{h}_{rn-1} \times \boldsymbol{a}_1\right) \\ \vdots & \vdots & \ddots & \ddots & \vdots \\ \|\boldsymbol{h}_{r1}\|\sin\phi_1 & 0 & \cdots & 0 & \hat{\boldsymbol{g}}_2 \cdot \left(\boldsymbol{h}_{r2} \times \boldsymbol{a}_1\right) \end{bmatrix} \begin{bmatrix} \dot{\theta}_n \\ \dot{\theta}_{n-1} \\ \vdots \\ \dot{\theta}_1 \end{bmatrix} = \begin{bmatrix} -\hat{\boldsymbol{g}}_n \cdot \left(\boldsymbol{h}_{rn} \times \boldsymbol{\omega}^{\mathrm{B/N}}\right) \\ -\hat{\boldsymbol{g}}_{n-1} \cdot \left(\boldsymbol{h}_{rn-1} \times \boldsymbol{\omega}^{\mathrm{B/N}}\right) \\ \vdots \\ -\hat{\boldsymbol{g}}_1 \cdot \left(\boldsymbol{h}_{r1} \times \boldsymbol{\omega}^{\mathrm{B/N}}\right) \end{bmatrix} \tag{4}$$

This expression is written without explicit basis vectors. Implementation would likely include a coordinate system based on Denavit-Hartenberg parameters or some other convenient rubric for parameterizing the forward kinematics. We also note here that if the rotor angular-momentum is the same from one CMG to the next, its magnitude can be factored out of this equation, resulting in a purely kinematical expression.

Solving these equations for $\dot{\theta}$ involves inverting an n×n matrix because these constraints specify each joint rate. However, it is clear that this matrix can be singular for certain joint alignments. As a demonstration, we represent them in the form of an (n-1)×(n-1) system of equations and a single scalar equation:

$$\begin{bmatrix} \hat{\boldsymbol{g}}_n \cdot \left(\boldsymbol{h}_{rn} \times \boldsymbol{a}_{n-1}\right) & \hat{\boldsymbol{g}}_n \cdot \left(\boldsymbol{h}_{rn} \times \boldsymbol{a}_{n-2}\right) & \cdots & \hat{\boldsymbol{g}}_n \cdot \left(\boldsymbol{h}_{rn} \times \boldsymbol{a}_1\right) \\ 0 & \hat{\boldsymbol{g}}_{n-1} \cdot \left(\boldsymbol{h}_{rn-1} \times \boldsymbol{a}_{n-2}\right) & \cdots & \hat{\boldsymbol{g}}_{n-1} \cdot \left(\boldsymbol{h}_{rn-1} \times \boldsymbol{a}_1\right) \\ \vdots & \ddots & \ddots & \vdots \\ 0 & \cdots & 0 & \hat{\boldsymbol{g}}_2 \cdot \left(\boldsymbol{h}_{r2} \times \boldsymbol{a}_1\right) \end{bmatrix} \begin{bmatrix} \dot{\theta}_{n-1} \\ \dot{\theta}_{n-2} \\ \vdots \\ \dot{\theta}_1 \end{bmatrix} = \begin{bmatrix} \|\boldsymbol{h}_{rn}\|\dot{\theta}_n \sin\phi_n - \hat{\boldsymbol{g}}_n \cdot \left(\boldsymbol{h}_{rn} \times \boldsymbol{\omega}^{\mathrm{B/N}}\right) \\ \|\boldsymbol{h}_{rn-1}\|\dot{\theta}_{n-1} \sin\phi_{n-1} - \hat{\boldsymbol{g}}_{n-1} \cdot \left(\boldsymbol{h}_{rn-1} \times \boldsymbol{\omega}^{\mathrm{B/N}}\right) \\ \vdots \\ \|\boldsymbol{h}_{r2}\|\dot{\theta}_2 \sin\phi_2 - \hat{\boldsymbol{g}}_2 \cdot \left(\boldsymbol{h}_{r2} \times \boldsymbol{\omega}^{\mathrm{B/N}}\right) \end{bmatrix} \tag{5}$$

$$\hat{\boldsymbol{g}}_1 \cdot \left(\boldsymbol{h}_{r1} \times \boldsymbol{\omega}^{\mathrm{B/N}}\right) = \|\boldsymbol{h}_{r1}\|\dot{\theta}_1 \sin\phi_1$$

Consider the case of $\sin\phi_1$=0. Here, the inboardmost joint rate $\dot{\theta}_1$ is undefined unless $\hat{\boldsymbol{g}}_1 \perp \left(\boldsymbol{h}_{r1} \times \boldsymbol{\omega}^{\mathrm{B/N}}\right)$ or $\boldsymbol{h}_{r1} \parallel \boldsymbol{\omega}^{\mathrm{B/N}}$, in which case $\dot{\theta}_1$ is merely unconstrained and can therefore take on any value. This principle can be extended for all of the joint angles, although simple expressions are not available (they involve the singular values of the matrix).

The fifth equation constrains the central-body rate such that the inboardmost joint requires zero power. The presence of this constraint forces the attitude-control systems engineer to consider an important question: given multiple kinematic chains (robotic arms), each of which may be attached to the central body, what is the best strategy for accommodating the minimum-power requirements of all of them simultaneously? One approach is to constrain either the joint rate θ_1 or the gimbal angle ϕ_1 of each arm so that the fifth equation is satisfied. However, doing so essentially prevents the innermost joint from moving to place the end effector in a desired trajectory; it also

introduces a constraint that cascades throughout the rest of the bodies, constraining their motion as well. The solution must weigh the power-minimization needs of all joints and the central body simultaneously with the combined attitude-control and joint-control commands to be executed. Absent the n^{th} constraint, the system has a single-degree-of-freedom null space within which maneuvers can take place with minimum energy. Since far more degrees of freedom are necessary for useful tasks, the control-design problem is to find the path that minimizes energy subject to a weighted combination of these constraints without necessarily satisfying them all exactly.

An alternative view of these constraints is that they provide a way to specify the central-body angular velocity $\boldsymbol{\omega}^{\text{B/N}}$ so that it minimizes the power for arbitrary joint velocities. This angular-velocity vector is regulated by the attitude-control system for the maintenance bot, and the operations concept may allow the use of the central body for energy-minimization. We emphasize, however, that this approach is efficient only if the power required to steer the central body in this fashion is less than what such steering saves in the joints.

To develop this law we represent the vectors' measure numbers such that the projection of some arbitrary vector $\boldsymbol{v}$ onto each of a set of basis vectors C is written as the 3×1 matrix ${}^{\text{C}}v$, i.e.,

$$ {}^{C}v = \begin{bmatrix} \boldsymbol{c}_1 \cdot \boldsymbol{v} & \boldsymbol{c}_2 \cdot \boldsymbol{v} & \boldsymbol{c}_3 \cdot \boldsymbol{v} \end{bmatrix}^{\text{T}} \tag{6} $$

For example, these basis vectors may conveniently describe the orientation of the central body relative to an object in the workspace to be manipulated. In any case, the central-body angular velocity in C coordinates ${}^{\text{C}}\omega^{\text{B/N}}$ can be specified in terms of arbitrary joint angular rates in a way that minimizes power as follows:

$$ {}^{C}\omega^{\text{B/N}} = \begin{bmatrix} -{}^{C}\hat{g}_n{}^{\text{T}}\,{}^{C}h_{rn} \\ -{}^{C}\hat{g}_{n-1}{}^{\text{T}}\,{}^{C}h_{rn-1} \\ \vdots \\ -{}^{C}\hat{g}_1{}^{\text{T}}\,{}^{C}h_{r1} \end{bmatrix}^{+} \begin{bmatrix} \|\boldsymbol{h}_{rn}\| \sin\varphi_n & {}^{C}\hat{g}_n \cdot \left({}^{C}h_{rn}{}^{\times}\,{}^{C}a_{n-1}\right) & {}^{C}\hat{g}_n \cdot \left({}^{C}h_{rn}{}^{\times}\,{}^{C}a_{n-2}\right) & \cdots & {}^{C}\hat{g}_n \cdot \left({}^{C}h_{rn}{}^{\times}\,{}^{C}a_1\right) \\ \|\boldsymbol{h}_{rn-1}\| \sin\varphi_{n-1} & 0 & {}^{C}\hat{g}_{n-1} \cdot \left({}^{C}h_{rn-1}{}^{\times}\,{}^{C}a_{n-2}\right) & \cdots & {}^{C}\hat{g}_{n-1} \cdot \left({}^{C}h_{rn-1}{}^{\times}\,{}^{C}a_1\right) \\ \vdots & \vdots & \ddots & \ddots & \vdots \\ \|\boldsymbol{h}_{r1}\| \sin\varphi_1 & 0 & \cdots & 0 & {}^{C}\hat{g}_2 \cdot \left({}^{C}h_{r2}{}^{\times}\,{}^{C}a_1\right) \end{bmatrix} \begin{bmatrix} \dot{\theta}_n \\ \dot{\theta}_{n-1} \\ \vdots \\ \dot{\theta}_1 \end{bmatrix} \tag{7} $$

where the superscript × indicates the skew-symmetric matrix equivalent of the cross-product operation, and the superscript + denotes the Moore-Penrose pseudoinverse. The angular-velocity vector's representation in C includes only three parameters; therefore, a robot with more than three links cannot experience minimum-energy dynamics. Instead, the pseudoinverse used in this expression provides a least-squares best ${}^{\text{C}}\omega^{\text{B/N}}$ given the possibly conflicting constraints. Again, the controls architecture may instead choose to weight this constraint for energy minimization relative to some other objective in defining the steering commands.

We emphasize that the singularity in this matrix is not directly related to the kinematic singularities associated with robotic systems, whereby certain joints align in a way that would demand unrealizable actuator forces. Instead, when the power mapping discussed here becomes singular, certain joints simply cannot be used to minimize power. The question of kinematic singularities is an interesting and relevant one, but it is the same for the maintenance bot as for any other robotic system. The same design principles of redundant joint degrees of freedom and singularity-avoidance apply here. The benefit of the maintenance bot's architecture is the use of CMGs as a ready means of limiting power but producing very high agility.

IV. Power

Here we provide a simple example that compares the low-power, high-agility features of the maintenance bot to other approaches. In this example, the maintenance bot consists of a central body and a three-link arm. For simplicity, each link's mass center is on its joint axis. Furthermore, the mass center of any system of outboard joints lies on the axis of the inboard joint, with the result that forces and mass-center motions are irrelevant. This principle is a worthy design goal, albeit difficult to achieve in practice (particularly for times when the manipulator is carrying a payload). Nevertheless, we argue that this simplification helps make the power comparison clearer for the sake of illustrating the concept's capabilities and is therefore justified in the context of this paper. For the same reason, products of inertia are taken to be zero. Other parameters in the example are listed in Table 1. The design on which these parameters are based is somewhat arbitrary; but it corresponds roughly to a system of about 1m in characteristic link length (about a 2 m radius workspace) and no more than 100 kg overall mass.

Table 1. Parameters for the Three-Link Example

Parameter	Value
Central Body Inertia	50 kg·m^2 in all axes
Link 1 inertia	10 kg·m^2 in all axes
Link 2 inertia	10 kg·m^2 in all axes
Link 3 inertia	10 kg·m^2 in all axes
CMG rotor momentum	50 Nms (Honeywell M50 CMG)
Link 1 CMG gimbal axes	[0 1 0] in Link 1 coordinates
Link 2 CMG gimbal axes	[0 0 1] in Link 2 coordinates
Link 3 CMG gimbal axes	[1 0 0] in Link 2 coordinates
RWA rotor inertia	0.08 kg·m^2 in all axes
CMG rotor inertia	0.04 kg·m^2 in all axes
CMG gimbal inertia	0.02 kg·m^2 in all axes
CMG rotor rate (constant)	6000 RPM
Reference Configuration	
Link 1 joint axis	[1 0 0] in central-body coordinates
Link 2 joint axis	[0 1 0] in central-body coordinates
Link 3 joint axis	[0 0 1] in central-body coordinates
Initial CMG pair 1 gimbal angle	0 (momentum aligned with Link 1 joint axis)
Initial CMG pair 2 gimbal angle	0 (momentum aligned with Link 2 joint axis)
Initial CMG pair 3 gimbal angle	0 (momentum aligned with Link 3 joint axis)

In this example we consider three architectures. To allow a fair comparison, we require that the bus remain inertially fixed in each case: i.e., any reaction torques from the robotic arms must be taken out by the base-body attitude control system (ACS).

1. The first case is what we have described as the baseline maintenance bot architecture: reactionless, CMG-driven joints. Each joint includes a scissored pair of 25 Nms CMGs (for a total capacity of 50 Nms). It turns out that the base body does not move (regardless of the motion of the arm), so the base-body ACS design is irrelevant here.
2. The second case is identical except that each scissored pair of CMGs is replaced by a 50 Nms reaction wheel (RWA). Once again, the base-body ACS is irrelevant.
3. The third case includes traditional direct- or geared-drive motors that actuate the joints. Reaction torques applied the base body are significant, and they are compensated by a high-bandwidth reaction-wheel based ACS. The ACS uses four RWAs that are identical to those on the joints and whose spin axes are $\left[\pm\frac{1}{2} \quad \pm\frac{1}{2} \quad \frac{\sqrt{2}}{2}\right]$ in base-body coordinates.

The joints' kinematics are varied numerically across a wide range in an effort to capture the worst-case power and nominal statistics. This variation forms a Monte Carlo analysis, where the joint angles, angular rate, angular acceleration, and angular jerk are given values within the limits shown in Table 2. We take these agility requirements to specify the joint kinematics, not the inertial kinematics. For example, the angular-rate limits apply to the joint, not the angular velocity magnitude of the link in an inertial frame. Thus, the end-effector agility is greater than that of a single link, up to twice the level shown in the table (e.g. 229 deg/sec), making the maintenance bot an extremely capable system. Another important point is that the CMG gimbal-motor control-loop bandwidth is taken to be much higher than the characteristic frequencies in the kinematics (e.g. the 2 rad/sec^3 jerk), which is a reasonable assumption. This point allows us to make the approximation that the CMGs achieve the prescribed kinematics instantaneously.

Table 2. Agility Requirements for the Maintenance Bot Monte Carlo Example

Parameter	Minimum Value	Maximum Value
Joint angle (3 independent values)	$-\pi$	π
Joint rate (3 independent values)	-2 rad/sec	2 rad/sec
Joint acceleration (3 independent values)	-2 rad/sec^2	2 rad/sec^2
Joint jerk (3 independent values)	-2 rad/sec^3	2 rad/sec^3

In this analysis the joint angles are always given uniform distributions. However, for rate, acceleration, and jerk two types of distributions are considered: a uniform distribution, meant to represent something like a "day in the life" of the maintenance bot, a statistically representative selection of maneuvers; and a simple maximum or minimum, used to identify the worst-case power across all joint configurations. In all cases, we report only the power required if the electromechanical systems involved were lossless. In fact, some additional multiplier (say 50%) should be added to account for various I^2R losses in harness and friction losses in bearings. This scale may not be quite the same for all systems but, it turns out, the savings are so great for the baseline architecture that the difference could not change the outcome of a trade study.

One rarely encounters a specification of jerk in this context. For the maintenance bot, there are several important reasons for such a requirement. Among them, jerk is a direct measure of the changing acceleration, and thus the frequency content of the loading on both the maintenance bot and its payload. Minimizing jerk reduces the systems-engineering effort in managing structural stiffnesses in the design and considering frequency-dependent coupled loads. However, requiring low jerk limits the bandwidth of the joint control. Jerk also limits the range of simultaneous rate and acceleration that can be achieved. For example, the maximum positive joint rate and the maximum positive joint acceleration cannot be applied simultaneously if there is a jerk limit because the acceleration must change over a finite time; and the rate limit would be exceeded during the period of negative jerk. Finally, the jerk is also directly related to the CMG gimbal acceleration. So, we have selected a jerk limit that seems to balance the demands of structural dynamics with the desire for high-speed joint kinematics. We emphasize that it is the methodology that is of greatest interest here; the specific values will be refined when maintenance-bot parameters are allocated from higher-level performance requirements.

In all cases we assume that there is no regenerative power transfer; that is, the power bus must be designed to handle a current load equivalent to the absolute value of the mechanical kinetic-energy change (and losses). One might develop a cross-strapped set of actuators, in which power required by one is extracted from another. However, one of the goals of the maintenance bot is to use comparatively high-TRL solutions. And because CMGs and reaction wheels have flown very successfully for decades, we propose no significant modifications to the Honeywell designs.

In case 1, the scissored-pair kinematics (ϕ and its derivatives) are found from momentum conservation for the kinematic chain, using the randomly selected kinematics from the Monte Carlo simulation:

$$\begin{aligned}
&\boldsymbol{I}_3 \cdot \overset{3}{\boldsymbol{\omega}}{}^{3/N} + \boldsymbol{\omega}^{3/\mathrm{N}} \times \boldsymbol{I}_3 \cdot \boldsymbol{\omega}^{3/\mathrm{N}} = \boldsymbol{\tau}_3 \\
&\boldsymbol{I}_2 \cdot \overset{2}{\boldsymbol{\omega}}{}^{2/N} + \boldsymbol{\omega}^{2/\mathrm{N}} \times \boldsymbol{I}_2 \cdot \boldsymbol{\omega}^{2/\mathrm{N}} = \boldsymbol{\tau}_2 - \boldsymbol{\tau}_3 \\
&\boldsymbol{I}_1 \cdot \overset{1}{\boldsymbol{\omega}}{}^{1/N} + \boldsymbol{\omega}^{1/\mathrm{N}} \times \boldsymbol{I}_1 \cdot \boldsymbol{\omega}^{1/\mathrm{N}} = \boldsymbol{\tau}_1 - \boldsymbol{\tau}_2 \\
&\boldsymbol{I}_B \cdot \overset{B}{\boldsymbol{\omega}}{}^{B/N} + \boldsymbol{\omega}^{B/\mathrm{N}} \times \boldsymbol{I}_B \cdot \boldsymbol{\omega}^{B/\mathrm{N}} = -\boldsymbol{\tau}_1
\end{aligned} \tag{8}$$

where B indicates parameters for the base body. However, with a non-moving base body (per our assumptions), we have

$$\begin{aligned}
&\boldsymbol{I}_1 \cdot \overset{1}{\boldsymbol{\omega}}{}^{1/N} + \boldsymbol{\omega}^{1/\mathrm{N}} \times \boldsymbol{I}_1 \cdot \boldsymbol{\omega}^{1/\mathrm{N}} = -\boldsymbol{\tau}_2 \\
&0 = -\boldsymbol{\tau}_1
\end{aligned} \tag{9}$$

The jerk for a given body indicates how this torque changes in time ($\overset{\mathrm{N}}{\boldsymbol{\tau}}_3$); e.g. for the third link,

$$\boldsymbol{I}_3 \cdot \overset{33}{\boldsymbol{\omega}}{}^{3/N} + 2\boldsymbol{\omega}^{3/\mathrm{N}} \times \boldsymbol{I}_3 \cdot \overset{3}{\boldsymbol{\omega}}{}^{3/\mathrm{N}} + \overset{3}{\boldsymbol{\omega}}{}^{3/\mathrm{N}} \times \boldsymbol{I}_3 \cdot \boldsymbol{\omega}^{3/\mathrm{N}} + \boldsymbol{\omega}^{3/\mathrm{N}} \times \left(\boldsymbol{\omega}^{3/\mathrm{N}} \times \boldsymbol{I}_3 \cdot \boldsymbol{\omega}^{3/\mathrm{N}}\right) = \overset{\mathrm{N}}{\boldsymbol{\tau}}_3 . \tag{10}$$

The momentum in the i^{th} scissored pair is

$$\boldsymbol{h}_{ri} = 2h_r \sin\phi_i \hat{\boldsymbol{a}}_i \,. \tag{11}$$

Solving for momentum along the $\boldsymbol{a}_i$ axis yields $\phi_i = \sin^{-1}\frac{h_{ri}}{2h_r}$. The torque it applies along the $\boldsymbol{a}_i$ axis leads to

$$\dot{h}_{ri} = 2h_r \cos\phi_i \dot{\phi}_i \quad \rightarrow \quad \dot{\phi}_i = \frac{\dot{h}_{ri}}{2h_r \cos\phi_i}, \tag{12}$$

and the time-varying torque (due to jerk) provides

$$\ddot{h}_{ri} = 2h_r\left(\cos\phi_i \ddot{\phi}_i - \sin\phi_i \dot{\phi}_i\right) \quad \rightarrow \quad \ddot{\phi}_i = \frac{\ddot{h}_{ri}}{2h_r \cos\phi_i} + \tan\phi_i \dot{\phi}_i \,. \tag{1}$$

From these parameters, the power required by the i^{th} CMG is

$$\begin{aligned} P_i = &\left(\Omega_r \hat{\boldsymbol{r}}_i + \dot{\phi}_i \hat{\boldsymbol{g}}_i + \boldsymbol{\omega}^{i/\mathrm{N}}\right)\cdot \boldsymbol{I}_r \cdot \left(\ddot{\phi}_i \hat{\boldsymbol{g}}_i + \overset{i}{\dot{\boldsymbol{\omega}}}{}^{i/\mathrm{N}} - \Omega_r \hat{\boldsymbol{r}}_i \times \dot{\phi}_i \hat{\boldsymbol{g}}_i - \left(\Omega_r \hat{\boldsymbol{r}}_i + \dot{\phi}_i \hat{\boldsymbol{g}}_i\right)\times \boldsymbol{\omega}^{i/\mathrm{N}}\right) + \\ &\left(\dot{\phi}_i \hat{\boldsymbol{g}}_i + \boldsymbol{\omega}^{i/\mathrm{N}}\right)\cdot \boldsymbol{I}_g \cdot \left(\ddot{\phi}_i \hat{\boldsymbol{g}}_i + \overset{i}{\dot{\boldsymbol{\omega}}}{}^{i/\mathrm{N}} - \dot{\phi}_i \hat{\boldsymbol{g}}_i \times \boldsymbol{\omega}^{i/\mathrm{N}}\right) \end{aligned} \tag{13}$$

where Ω_r is the CMG rotor rate, $\hat{\boldsymbol{r}}_i$ is the rotor spin axis, $\dot{\phi}_i$ is the gimbal rate, $\boldsymbol{\omega}^{i/\mathrm{N}}$ is the i^{th} link's angular velocity in an inertial frame N, $\boldsymbol{I}_r$ is the rotor inertia dyadic, $\ddot{\phi}_i$ is the gimbal acceleration, $\overset{i}{\dot{\boldsymbol{\omega}}}{}^{i/\mathrm{N}}$ is the angular acceleration of the i^{th} link in an i-fixed frame, and $\boldsymbol{I}_g$ is the gimbal inertia dyadic.

The power is considerably simpler in the case of the reactionless RWA architecture. Beginning with the angular momentum for each link, we simply compute

$$h_{ri} = \hat{\boldsymbol{a}}_i \cdot \boldsymbol{I}_i \cdot \boldsymbol{\omega}^{i/\mathrm{N}} \,. \tag{14}$$

Similarly, the RWA torque is simply

$$\tau_{ri} = \hat{\boldsymbol{a}}_i \cdot \left(\boldsymbol{I}_i \cdot \overset{i}{\dot{\boldsymbol{\omega}}}{}^{i/\mathrm{N}} + \boldsymbol{\omega}^{i/\mathrm{N}} \times \boldsymbol{I}_i \cdot \boldsymbol{\omega}^{i/\mathrm{N}}\right). \tag{15}$$

The power for each RWA is then

$$P_i = \tau_{ri}\frac{h_{ri}}{I_r}, \tag{16}$$

where we have taken advantage of the fact that the rotor inertia is the same for all axes (by the assumptions explained above).

In the third case, we compute the time rate of change in the three-link system's kinetic energy E_{joints} and take that power to be required of the joint motors, whatever they may be. Then, the net momentum of the outboard joints must be absorbed by the ACS RWAs (assuming no external torques on the maintenance bot), as must the torque of the three-link system transmitted via the inboard joint:

$$P = \dot{E}_{joints} + \dot{E}_{ACS} = \sum_{i=1}^{3} \boldsymbol{\omega}^{i/\mathrm{N}} \cdot \boldsymbol{I}_i \cdot \overset{i}{\boldsymbol{\omega}}{}^{i/\mathrm{N}} + \dot{E}_{ACS} \tag{17}$$

The power due to ACS activity is then simply the shaft power for each of the four RWAs. Given the matrix A of spin axes (as defined in Table 1),

$$A = \begin{bmatrix} 0.5 & -0.5 & 0.5 & -0.5 \\ 0.5 & 0.5 & -0.5 & -0.5 \\ \frac{\sqrt{2}}{2} & \frac{\sqrt{2}}{2} & \frac{\sqrt{2}}{2} & \frac{\sqrt{2}}{2} \end{bmatrix}, \tag{18}$$

the four RWAs' angular momenta $h_{acs,i}$ may be found from the base-body angular momentum h_{base} via

$$\begin{bmatrix} h_{acs,1} \\ h_{acs,2} \\ h_{acs,3} \\ h_{acs,4} \end{bmatrix} = A^{\mathrm{T}}\left(AA^{\mathrm{T}}\right)^{-1} h_{base}, \tag{19}$$

The same result applies to reaction-wheel torques $\tau_{acs,i}$. Some straightforward calculations provide an estimate of the wheel power for the array. Here, the absolute values (not the vector norms) are taken for each RWA spin rate because of our requirement that there is no flywheel-style energy storage, and that all power must come from the base body power bus or be shunted into a resistor.

V. Conclusions

The results of the Monte Carlo analysis for day-in-the-life statistics are shown in Figure 6. The first case, the baseline maintenance bot, requires about 151 W for typical operations, despite its extraordinarily high agility. In contrast, the reactionless RWA case requires about 3300 W, and the traditional joint-drive architecture requires about 7200W.

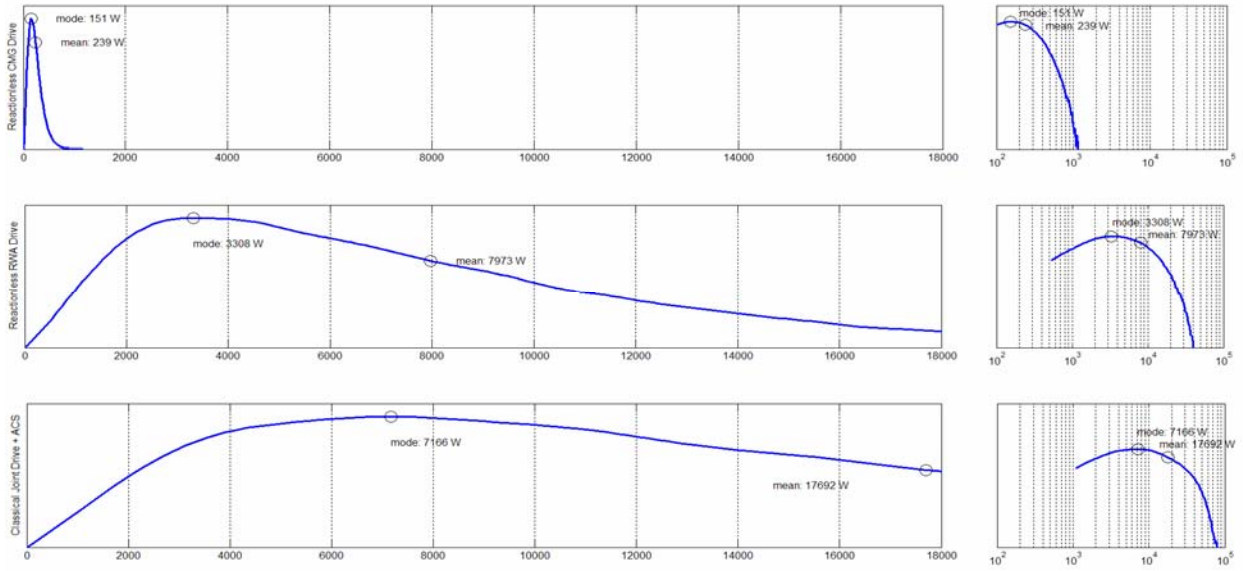

Input Power, W

Figure 6. Day in the Life Probability Density for Electromechanical Power: Three Cases, Both Linear and Logarithmic Scales Shown.

The worst-case analysis (maximum rate, acceleration, and jerk, for all values of joint angle) reveals a similar trend. The bar graph in Figure 7 shows that the CMG-based reactionless architecture requires between 200 W and 1500 W for worst-case kinematics over the range of joint angles, while the RWA-based architecture requires up to 70kW. The traditional joint-drive architecture demands an astounding 118 kW.

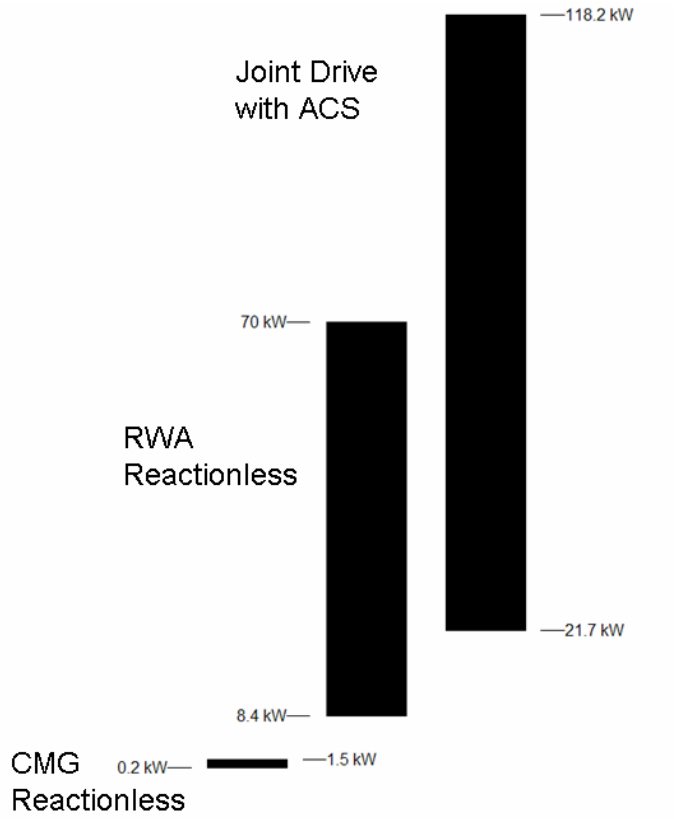

Figure 7. Range of Minimum and Maximum Power Required (Kinematic Limits, All Joint Angles) for All Three Cases

The key conclusion is that the CMG-based maintenance-bot architecture can radically outperform other systems in power for high-agility maneuvers. Furthermore, this architecture opens up a large trade space for power vs. agility, allowing highly effective maintenance bots to be incorporated for relatively low power-specific mass. Or, for a given mass, the maintenance bot can withstand more demanding operations for longer than competing architectures.

Acknowledgments

The author would like to thank Ms. Michele Carpenter and Professor Andy Ruina, both of Cornell University, for valuable discussions on this subject.

References

[1] Honeywell International, *M50 Product information Sheet,* URL http://www.honeywell.com/sites/aero/Pointing-Momentum-Control.htm [cited August 11, 2005].
[2] Quartararo, R., Course Notes, *Introduction to Spacecraft Attitude Control*, University of Southern California, 2003.
[3] Fattah, A., and Agrawal, S., 2005, "Design and Simulation of a Class of Spatial Reactionless Manipulators", Robotica, Vol. 23, No. 1, pp.75-81.
[4] Peck, M. A., "Estimation of Wheel and CMG Alignments from On-Orbit Telemetry," *2001 Flight Mechanics Symposium*, 2001.